Dynamic Nuclear Orientation of Co^{60}†

M. ABRAHAM,* C. D. JEFFRIES, AND R. W. KEDZIE‡
Department of Physics, University of California, Berkeley, California
(Received September 8, 1959)

An experiment to dynamically orient Co^{60} nuclei is described, using a method discussed in the preceding paper; the orientation is detected by the γ-ray anisotropy. The Co^{60} is contained as Co^{++} ions in magnetically isotropic sites of a single crystal of $La_2Mg_3(NO_3)_{12}\cdot 24D_2O$ at 1.5°K and in a field of ~1500 gauss. Application of an rf field at a frequency $\nu\sim 9400$ Mc/sec produces an orientation when the forbidden hfs transitions $W_2(M, m \rightarrow M\pm 1, m\mp 1)$ are induced; m and M are the magnetic quantum numbers of the Co^{60} nucleus and the Co^{++} ion, respectively. With a few milliwatts of microwave cavity power a steady-state dynamic nuclear orientation is reached in a time less than a few seconds yielding an anisotropy $\epsilon\sim 1\%$, smaller by a factor 2.7 than the theoretical optimum value. No γ-ray anisotropy is observed when the allowed hfs transitions $W_1(M, m \rightarrow M\pm 1, m)$ are induced. Also, no γ-ray anisotropy is found upon inducing either W_1 or W_2 for Co^{++} located in the magnetically anisotropic sites in the crystal. All the above observations are in general agreement with the theoretical expectations. An anomalous orientation of Co^{60} is observed when the allowed hfs transitions of abundant stable Co^{59} in the same crystal are strongly induced. This is explicable in terms of a mutual spin-flip process between the two systems.

I. INTRODUCTION

THIS paper presents the details of an experiment to dynamically orient 5.3 yr Co^{60} nuclei by the methods discussed in the preceding paper,[1] which we refer to as I, and which notation we follow. The experiment has been briefly described earlier[2] and consists in saturating certain (forbidden) transitions in the paramagnetic resonance spectra of divalent Co^{60} ions in a crystal and observing the resulting γ-ray anisotropy.

We have used the deutrated double nitrate crystal $La_2Mg_3(NO_3)_{12}\cdot 24D_2O$, in which a small fraction of the Mg^{++} ions have been replaced by Co^{++} ions. Paramagnetic resonance was first observed, for the hydrated crystal, by Trenam,[3] who found two magnetically unequivalent sites for Co^{++} ions, designated as site I and site II, with the relative populations I:II$\cong$1.6:1. The spectra of the deutrated and the hydrated crystals are very similar and can be fitted to a spin Hamiltonian of the form of Eqs. (5) and (6) of I, with $S=\frac{1}{2}$. Our experimental values for the constants in the spin Hamiltonian are given in Table I. The values $A(Co^{59})$ and $B(Co^{59})$ were determined directly from the paramagnetic resonance spectra of stable Co^{59}, for which $I=\frac{7}{2}$. For Co^{60}, $I=5$, and we obtained $A(Co^{60})$ and $B(Co^{60})$ from the measured value $A(Co^{60})/A(Co^{59})=0.573\pm 0.001$ in the Tutton salt,[4] by assuming that the ratio $A(Co^{60})/A(Co^{59})=B(Co^{60})/B(Co^{59})$ is a constant for all paramagnetic salts; this is well justified to the precision involved in the present experiment. The energy level diagram, the rf-induced transition probabilities, and the relaxation transitions for Co^{60} in the double nitrate crystal would be as in Figs. 2 and 6 in I, generalized to spin $I=5$. We arbitrarily assume, for the present, that the hfs constant A is positive.

Co^{60} decays by β^- emission, followed by two γ-rays (1.17, 1.33 Mev) in cascade to the ground state of Ni^{60}: $5(\beta 1)4(\gamma 2)2(\gamma 2)0$. The γ rays are so prompt ($\sim 10^{-11}$ sec) that we are justified in neglecting reorientation effects in the intermediate states. Then the angular distributions of the two γ rays are identical and the dynamic anisotropy is given by Eq. (50), of I, where $\alpha_2=-1/63$, $\alpha_4=-1/735$, and the orientation parameters p_2' and p_4' are determined by the dynamic equilibrium populations of the magnetic states of Co^{60}.

II. APPARATUS AND EXPERIMENTAL PROCEDURES

Single crystals of $(Co, Mg)_2La_3(NO_3)_{12}\cdot 24D_2O$ were grown in a desiccator at constant temperature (~20°C) by seeding an almost saturated heavy water solution of $La_2Mg_3(NO_3)_{12}$ to which had been added pile-produced Co^{60} in the form of $Co(NO_3)_2$. A typical crystal (~10 hours growing-time) weighed ~300 mg, contained ~2 mC of Co^{60} activity, and had the isotopic abundance ratios $Mg:Co^{59}:Co^{60}\approx 10^4:60:1$. The crystals grow in thin hexagonal plates with the crystalline z' axis perpendicular to the plate.

After being coated with Krylon plastic the crystal sample, containing both Co^{59} for paramagnetic reso-

TABLE I. Measured values of spin Hamiltonian constants for Co^{++} in $La_2Mg_3(NO_3)_{12}\cdot 24D_2O$ at 4.2°K; $\nu=9400$ Mc/sec.

	Site I	Site II
$g_{\parallel}$	4.28±0.05	7.9±0.1
$g_{\perp}$	4.45±0.05	2.34±0.05
$A(Co^{59})$	0.0091±0.0002 cm^{-1}	0.0315±0.0005 cm^{-1}
$B(Co^{59})$	0.0106±0.0002 cm^{-1}	very small
$A(Co^{60})$	0.0052 cm^{-1}	0.01805 cm^{-1}
$B(Co^{60})$	0.00607 cm^{-1}	very small

† Supported in part by the U. S. Atomic Energy Commission.
* Present Address: The Clarendon Laboratory, Oxford, England.
‡ Present Address: Polychem Department, DuPont Experimental Station, Wilmington, Delaware.
[1] C. D. Jeffries, preceding paper [Phys. Rev. **117**, 1056 (1960)].
[2] M. Abraham, R. W. Kedzie, and C. D. Jeffries, Phys. Rev. **106**, 165 (1957).
[3] R. S. Trenam, Proc. Phys. Soc. (London) **A66**, 118 (1953).
[4] W. Dobrowolski, R. V. Jones, and C. D. Jeffries, Phys. Rev. **101**, 1001 (1956).

nance measurements and Co^{60} for γ-ray measurements, was mounted in the resonant cavity of a 3-cm microwave paramagnetic resonance spectrometer. The cavity is a silvered glass cylinder operating in the TE_{111} mode, connected to a magic-T bridge through a rotating waveguide joint, permitting rotation of the cavity and hence the angle between z' and the dc magnetic field H. A mode supressor fixes the direction of the major component of the cavity rf field H_1, allowing for orientations between these approximate extremes: (a) $z'\|H\perp H_1$ and (b) $z'\perp H\|H_1$. Thus orientation (a) will preferentially induce the allowed transitions W_1 of Eq. (21) in I, while orientation (b) preferentially induces the forbidden transitions W_2 and W_3 of Eqs. (25) and (26) in I. Because of the curvature of the rf flux lines, however, this is only approximately so, since for any cavity orientation there will be nonvanishing components of H_1 both parallel and perpendicular to H.

The cavity is immersed in and filled with liquid helium, pumped to 1.5°K. The H field is provided by an electromagnet with 12-in. diameter pole faces and a $5\frac{1}{2}$-in. gap. The rf field H_1 is supplied by a klystron coupled to an arm of the magic T, furnishing up to $\sim$100 mw of power to the cavity, corresponding to $H_1\sim 0.1$ gauss. Paramagnetic resonance of the abundant Co^{59} is observed in the usual way by modulation of H at 100 kc/sec or at 80 cps and recording on a paper tape the derivative of either the absorption or dispersion as H is slowly varied.

The Co^{60} γ rays are detected by two identical NaI(Tl) scintillation crystals, 1 in. in diameter and 1 in. long, mounted in the magnet gap at a distance of $1\frac{3}{4}$ in. from the sample crystal in directions parallel and perpendicular to H, respectively. The scintillation crystals are each connected by Lucite light pipes, 18 in. long and $1\frac{1}{4}$ in. in diameter, to matched photomultiplier tubes (RCA type 6655), well outside the magnet gap. The phototubes are magnetically shielded and aligned in such a way that variation of H in the gap from, say, 3000 gauss to 1000 gauss does not change the γ counting rate by more than $\sim 0.2\%$ in the absence of dynamic nuclear orientation. The two phototubes are supplied by a common regulated power supply ($\sim$1200 volts) but with individual voltage adjustment potentiometers. The anode currents are each integrated with a capacitor across the anode resistor (time constant $\sim$10 sec), yielding average voltages $G(0)$ and $G(\pi/2)$, proportional, respectively, to the total γ-ray intensity in directions parallel and perpendicular to H. The supply voltages are so balanced that $G(0)=G(\pi/2)=G_0$ in the absence of dynamic nuclear orientation. The voltage difference $G(\pi/2)-G(0)$ is recorded on a paper tape as the field is slowly varied, thus directly plotting the dynamic anisotropy $\epsilon=[G(\pi/2)-G(0)]/G_0$ as a function of H.

We note that this simple anisotropy detector does not allow for discrimination of γ-ray energies by pulse-height selection. However it is adequate in the present experiment, where there is a simple decay scheme; it is automatic and operates at a high counting rate ($\sim 10^6$ sec^{-1}), allowing anisotropies as small as 0.1% to be detected in a moderate counting time.

III. RESULTS AND CONCLUSIONS

A. Orientation $z'\perp H\|H_1$

For Co^{++} ions in site I, Fig. 1(a) shows the recorded paramagnetic resonance hfs spectrum of Co^{59} in a double nitrate crystal so oriented that $z'\perp H\|H_1$, approximately. The temperature was held at 1.5°K, the microwave frequency at $\nu=9400$ Mc/sec, while the field H was slowly swept from 1700 to 1200 gauss by a motor drive. The line shape is the derivative of the dispersion, distorted by modulation effects. $2I+1=8$ lines are seen and are clearly the usual allowed transitions W_1; this is evidenced by their correspondence with Fig. 1(b), which shows the calculated positions of these lines as given by Eq. (12) in I to second order. We note that even though $H_1\|H$, approximately, there is still a sufficient component $H_1'\perp H$ to make $W_1>W_2$. The high field line at 1636 gauss corresponds to $W_1(\frac{1}{2},-5\rightarrow-\frac{1}{2},-5)$, etc. The line width $\Delta H\sim 25$ gauss. The thermal relaxation time $T_1=w_1^{-1}$ was estimated to be of the order of 10^{-1} sec from the transient response of the signals.

Figure 1(c) is the observed γ-ray anisotropy of Co^{60} in the same crystal, recorded simultaneously with Fig. 1(a) on the same H scale. The maximum anisotropy observed is about 1%. Figure 1(d) presents, on the same ordinate and abscissa scales, the anisotropy given by Eq. (50) in I, with p_2' and p_4' calculated under the following assumptions. The solid lines in Fig. 1(d) give the positions and intensities of the steady state anisotropy assuming that the relaxation transitions $bw=cw=0$ in Fig. (6) of I, and that the allowed transitions W_1 are individually saturated in turn as H is varied. The dashed lines in Fig. 1(d) give the anisotropy when the forbidden transitions W_2 are individually saturated in turn. We neglect the anisotropy due to saturation of the W_3 transitions, since $W_3=(A-B)^2/(A+B)^2W_2\approx 2\times 10^{-3}W_2$. We have assumed that the fraction 1.6/2.6 of the Co^{60} nuclei is in ionic site I, the anisotropy being reduced proportionately, since the remaining fraction is in nonresonant site II. The positions of the lines in Fig. 1(d) were precisely located with respect to those of Fig. 1(b) using the known ratios $A(Co^{60})/A(Co^{59})$ and Eqs. (12) and (14) in I; an exact knowledge of H or the crystal orientation is not necessary.

A comparison of Fig. 1(c) with 1(d) shows that the observed anisotropy is in good agreement in both position and in sign with that calculated for saturation of the forbidden transitions W_2. The magnitude is about 2.7 times less than that calculated, but the relative intensities are in reasonable agreement as shown in Table II. Saturation of the allowed transitions W_1 produces an anisotropy much less than that calculated; in fact no anisotropy lines were detected, except for the small high-field line in Fig. 1(c).

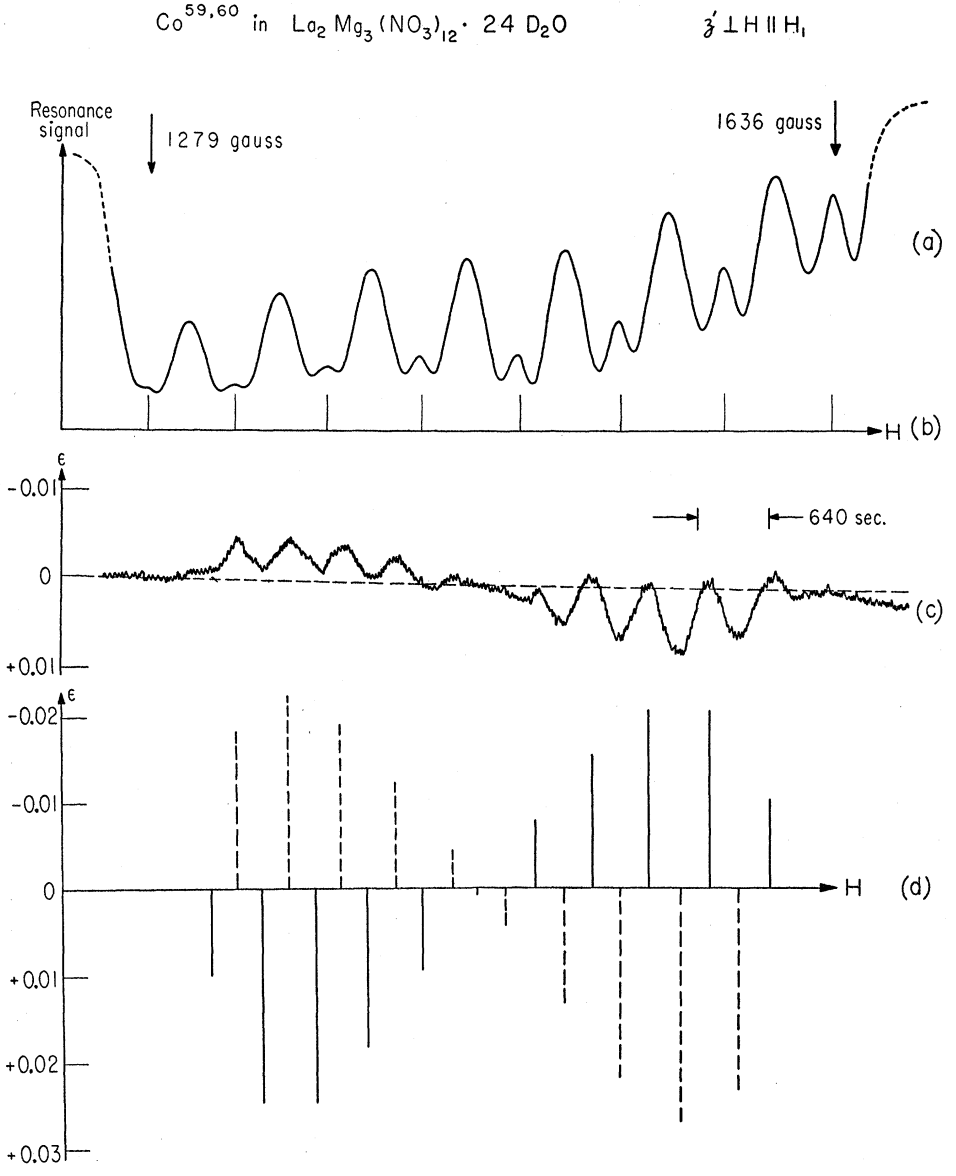

FIG. 1. (a) Paramagnetic resonance hfs spectrum of Co^{59} (site I ions) in $La_2Mg_3(NO_3)_{12}\cdot 24D_2O$ at 9400 Mc/sec and 1.5°K, so oriented that the crystal axis z' is perpendicular to the dc field H, which is parallel to the major component of rf field H_1; (b) calculated position of allowed Co^{59} transitions; (c) observed γ-ray anisotropy ϵ of Co^{60} in the same crystal; (d) calculated (ideal) anisotropy obtainable by saturation of allowed transitions W_1 (solid lines) or forbidden transitions W_2 (dashed lines).

There are many independent reasons why the observed anisotropy may be less than that calculated, besides insufficient rf field (which we do not believe to be the reason here). We have assumed $c=0$ and $b=0$ and, as discussed in I, if b approaches f or if c approaches f, this will appreciably reduce the anisotropy obtainable by saturating W_1, whereas b must become comparable to unity before the anisotropy due to saturation of W_2 is reduced appreciably. Also, γ-ray scattering can easily reduce the observed anisotropy by a factor two. We note further that if the resonance line width ΔH is due to inhomogeneous broadening,[5] i.e., "thermally" isolated spin packets, then only a small fraction of order $H_1/\Delta H \sim 10^{-3}$ of the sample can be saturated, reducing the anisotropy proportionately. This cannot be the case in the present experiments, however, since the observed anisotropy is only 2.7 times less than the ideal theoretical maximum; the experiments show, in fact, that the spin packets are brought into thermal contact in a time less than a few seconds by some kind of spectral diffusion process.[6,7] The whole line becomes saturated in the steady state. The anisotropy was found to be independent of the modulation field.

The observed anisotropy did not noticeably change for variations of cavity power over the range ~1 mw to ~50 mw. In some runs at temperatures $T \sim 1.3$°K the cavity power could be reduced to a few microwatts

[5] A. M. Portis, Phys. Rev. **91**, 1072 (1955).

[6] A. M. Portis, Phys. Rev. **104**, 584 (1956).

[7] N. Bloembergen, S. Shapiro, P. S. Pershan, and J. O. Artman, Phys. Rev. **114**, 445 (1959).

TABLE II. Relative intensities of γ-ray anisotropy lines, Fig. 1(c) and (d), normalized to 100 for the $W_2(\frac{1}{2}, -4 \rightarrow -\frac{1}{2}, -3)$ transition.

Observed	-73 ± 7	-72 ± 7	-66 ± 7	-48 ± 5	-19 ± 2	$+16\pm2$	$+54\pm6$	$+73\pm7$	$+100\pm10$	$+71\pm9$
Calculated	-67	-83	-71	-46	-16	$+16$	$+50$	$+81$	$+100$	$+87$

without reducing the anisotropy. Sweeping the H field four times more slowly than the indicated rate in Fig. 1 did not change the observed anisotropy. If H were fixed at the value for an anisotropy peak and the rf field H_1 switched off, the anisotropy decayed to zero in the time constant of the photocurrent integrating circuit, which could be made as short as $\sim$10 sec. Switching H_1 on restored the anisotropy in the same time, which may be regarded as an upper limit to the time required for the populations to approximately reach their steady-state dynamic equilibrium values. A lower limit to the relaxation time $(fw)^{-1}$ is obtained from the condition required to saturate the levels: $(fw) \leqq W_{2)\min} \sim 10$ sec^{-1}, where $W_{2)\min}$ is the transition probability calculated from Eq. (25) in I for the lowest cavity powers used ($\sim$1 mw).

The paramagnetic resonance hyperfine structure of Co^{59} in site II was observed at a field of about 3000 gauss and consisted of several nearly superposed lines ($B \approx 0$), which spread apart as the orientation $z' \perp H$ was changed by a few degrees. No dynamic γ-ray anisotropy was observed for Co^{60} in site II, probably because $W_2 \approx W_3$ and these two types of forbidden transitions are nearly superposed, giving equal and opposite anisotropies, which cancel.

We have arbitrarily assumed A to be positive and if now A is taken negative, this will not change the positions of the lines in Fig. 1(d), or their relative intensities

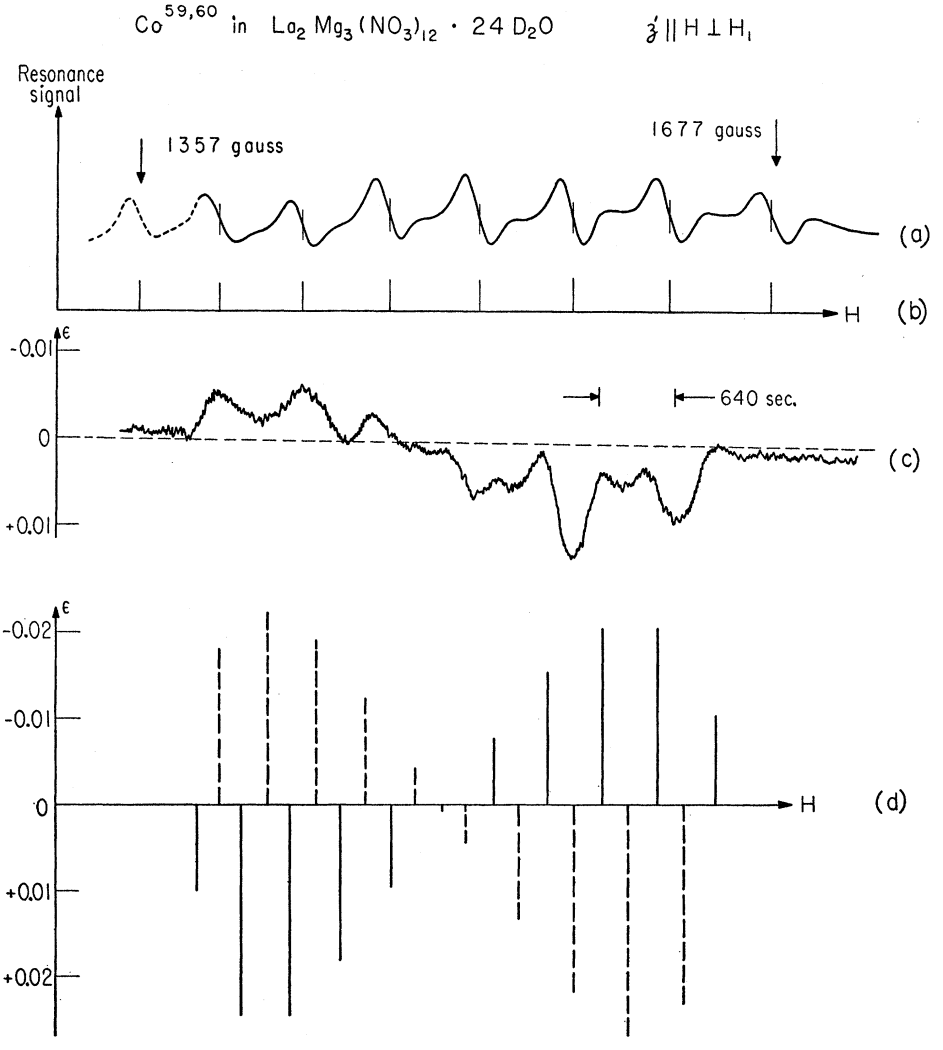

FIG. 2. (a) Paramagnetic resonance hfs spectrum of Co^{59} (site I ions) in $La_2Mg_3(NO_3)_{12} \cdot 24D_2O$ at 9400 Mc/sec and 1.5°K, so oriented that the crystal axis z' is parallel to the dc field H, which is perpendicular to the rf field H_1; (b) calculated positions of allowed Co^{59} transitions; (c) observed γ-ray anisotropy ϵ of Co^{60} in the same crystal; (d) calculated (ideal) anisotropy obtainable by saturation of allowed transitions W_1 (solid lines) or forbidden transitions W_2 (dashed lines).

as long as the dynamic anisotropy $\ll$ static anisotropy. The second order enhancement of the high-field anisotropy lines over the low-field anisotropy lines is independent of the sign of $A(Co^{60})$.

B. Orientation $z' \| H \perp H_1$

For the almost isotropic site I ions, the essential fact for this orientation is that the rf field is now so directed as to considerably increase the ratio W_1/W_2 over its value in case A above. For the same crystal the experimental results are shown in Fig. 2, where (a), (b), (c), and (d) represent the corresponding quantities in Fig. 1, except that the paramagnetic resonance line shape (a) is now the derivative of the absorption. It is clear from the sign of the observed anisotropy that the nuclear orientation is again due to the saturation of the forbidden transitions W_2. No anisotropy due to saturation of the W_1 transitions is detectable. The relative intensities and positions of the anisotropy lines do not agree well with those calculated, however, and a careful examination shows that a $W_2(Co^{60})$ line [Fig. 2(d)] which happens to lie near a $W_1(Co^{59})$ line [Fig. 2(b)] results in an anisotropy line [Fig. 2(c)] which is enhanced and even slightly shifted in position toward the $W_1(Co^{59})$ line.

This anomalous effect can be explained in terms of a spin-spin coupling between a pair of Co^{60} hfs levels (α system) and a pair of Co^{59} hfs levels (β system). Since the abundance ratio $Co^{60}:Co^{59} \approx 1:60$, it is probable that each member of the α system in the crystal lattice has several members of the β system as its closest magnetic neighbors. We have said that the observed anisotropy is due to saturation of the $W_2(Co^{60})$ transitions; this means, more precisely, an equalization of populations of the pair of levels $\psi_\alpha(\frac{1}{2},m_\alpha)$ and $\psi_{\alpha'}(-\frac{1}{2}, m_\alpha+1)$. In the event that the transition probability $W_2(Co^{60})$ is relatively small and unable to establish $N_\alpha \approx N_{\alpha'}$, then other processes which may equalize these populations become important, such as the following one, discussed in detail by Bloembergen, Shapiro, Pershan, and Artman.[7] The dipolar coupling between system α and system β will provide matrix elements for the mutual spin flip process: $\psi_\alpha(\frac{1}{2},m_\alpha) \rightarrow \psi_{\alpha'}(-\frac{1}{2}, m_\alpha+1)$ simultaneously with $\psi_{\beta'}(-\frac{1}{2}, m_\beta) \rightarrow \psi_\beta(\frac{1}{2},m_\beta)$. Energy will be conserved, or very nearly so, if $E_\alpha - E_{\alpha'} = h\nu_\alpha \approx h\nu_\beta = E_\beta - E_{\beta'}$. Suppose that an rf field is applied to strongly induce $W_1(Co^{59})$ transitions, i.e., to equalize the populations $N_\beta = N_{\beta'}$. Then, if thermal relaxation processes are not too strong, the population equalization $N_\alpha \approx N_{\alpha'}$ may be approximately established, in a "cross-relaxation" time T_{21},[7] which in the present case could be as short as 10^{-1} sec. That is, rf saturation of the allowed transition $W_1(Co^{59})$ will, in effect, "saturate" a nearlying level $W_2(Co^{60})$ transition, i.e., produce the same γ-ray anisotropy. This anomalous effect is superimposed on the direct effect due to rf-induced $W_2(Co^{60})$ transitions.

Comparison of Fig. 2(b) and (d) shows that six of the Co^{60} forbidden lines lie, by chance, very close to Co^{59} allowed lines. These give rise to the major anisotropy peaks, probably by the above process. The smaller anisotropy peaks, on the high-field side, lie in between Co^{59} lines and are probably due to the direct process; they disappear first at lower cavity powers, leaving only six anisotropy peaks near the Co^{59} lines. Although this explanation is only qualitative it is consistent with the observation, in A above, that the whole resonance line becomes saturated, very likely by a similar spin-flip process. Clearly this process could be a source of confusion in measuring nuclear moments of radionuclei by dynamic nuclear orientation: the γ-ray anisotropy pattern would tend to correspond to the hfs pattern of a stable isotope if it were relatively abundant. Conversely, it affords the observation of magnetic resonance of stable isotopes by a γ-ray detector.

No γ-ray anisotropy of Co^{60} ions in site II was observed, probably because for the orientation $z' \| H$, $W_2 \propto (B/H)^2$ and B is too small.

Not all crystals were "good," i.e., for both this orientation and that of A above we failed to observe a dynamic anisotropy for Co^{60} in several double nitrate crystals. In other cases an anisotropy was observed but not resolved into the peaks, e.g., as in Fig. 1(c); instead, a curve showing only one broad negative peak at high field, crossing over to a broad positive peak at lower fields, was observed. This behavior was also observed for 72-day Co^{56} and 72-day Co^{58} in the double nitrate. These failures were generally associated with either a poor crystal specimen, or else with extraneous paramagnetic impurities (Ni^{++} in Co^{58}; Ce^{+++} in the La) or else with excessive amounts of stable Co^{59}. No doubt spectral diffusion effects which equalize the populations of several adjacent hfs levels are important processes in these cases. Radiation damage to the crystal at the levels used here ($\sim$1 Mc) is probably not important, since we have observed that a "good" crystal, giving an anisotropy as in Fig. 1(c), gave a comparable anisotropy under the same conditions six months later, having been stored at room temperature in the meantime.

No dynamic γ-ray anisotropy was observed for Co^{60} ions grown in a single crystal of the Tutton salt $Zn(NH_4)_2(SO_4)_2 \cdot 6H_2O$. Although the paramagnetic anisotropy $A/B \sim 12$ is not as large as for site II in the double nitrate, this failure may be due to similar reasons.